

## Article

# Experimental Study of Mechanical Behavior of Dry-Stone Structure Contact <sup>†</sup>

Iriex Costa <sup>1,\*</sup>, Joan Llorens <sup>1</sup>, Miquel Àngel Chamorro <sup>1</sup>, Joan Fontàs <sup>1</sup>, Jordi Soler <sup>1</sup>, Ester Gifra <sup>1</sup> and Nathanaël Savalle <sup>2</sup>

<sup>1</sup> Departament d'Arquitectura i Enginyeria de la Construcció (DAEC), Universitat de Girona, Escola Politècnica Superior (EPS), 17003 Girona, Spain; joan.llorens@udg.edu (J.L.); mangel.chamorro@udg.edu (M.À.C.); joan.fontas@udg.edu (J.F.); jordi.soler@udg.edu (J.S.); ester.gifra@udg.edu (E.G.)

<sup>2</sup> Institut Pascal, Université Clermont Auvergne, Clermont Auvergne INP, CNRS, F-63000 Clermont-Ferrand, France; nathanael.savalle@uca.fr

\* Correspondence: iriex.costa@udg.edu

<sup>†</sup> This paper is an extended version of our paper published in Costa, I.; Llorens, J.; Chamorro, M.À.; Fontàs, J.; Soler, J.; Gifra, E.; Savalle, N. Experimental study of mechanical behaviour of dry-stone structures contact. In Proceedings of the Rehabend 2024, Gijon, Spain, 5–9 May 2024.

**Abstract:** Dry-stone structures are traditional constructions that are present everywhere around the world, with their stability working mostly by gravity. Contrarily to their in-plane behavior, their out-of-plane response is very brittle and is fully controlled by the geometry, as well as the contact properties, between units (stones). Two main local failure modes of dry-joint contact are identified to lead to the global failure of the structure: (i) sliding and (ii) joint opening. Most of the existing studies investigated full structures to obtain the global response and/or couplet only, with the aim of only characterizing the contact. The present experimental work studies the effect of sliding and joint opening between stones at different scales: couplets, structures made of a few (up to five) blocks, and full walls, as well as varying the way the masonry units are assembled within a single structure. Different stones are employed to quantify potential differences. All the structures are loaded up to the collapse with a tilting table to induce out-of-plane actions. Repeatability tests are also conducted to better understand the effect of contact variability. This study unveils that the heterogeneity of the dry-joint contact, as well as the repartition of the blocks, affects the global response (both in terms of load capacity and failure mode). It also confirms that the most critical local failure mode is produced by the joint opening.

**Keywords:** masonry; dry stone; retaining walls; pseudo-static; tilting tests



**Citation:** Costa, I.; Llorens, J.; Chamorro, M.À.; Fontàs, J.; Soler, J.; Gifra, E.; Savalle, N. Experimental Study of Mechanical Behavior of Dry-Stone Structure Contact.

*Buildings* **2024**, *14*, 3744. <https://doi.org/10.3390/buildings14123744>

Academic Editor: Grzegorz Ludwik Golewski

Received: 30 September 2024

Revised: 12 November 2024

Accepted: 18 November 2024

Published: 25 November 2024



**Copyright:** © 2024 by the authors. Licensee MDPI, Basel, Switzerland. This article is an open access article distributed under the terms and conditions of the Creative Commons Attribution (CC BY) license (<https://creativecommons.org/licenses/by/4.0/>).

## 1. Introduction

Masonry has been one of the primary construction techniques for centuries, providing structural solutions for everything from monumental edifices to practical rural infrastructure. Historical landmarks, such as the Parthenon, the pyramids, the Colosseum, and the Segovia aqueduct, exemplify the use of dry-joint masonry—structures that have stood the test of time, relying on the stability and integrity of stone or brick units assembled without mortar [1]. The use of dry-joint techniques is not limited to grand monuments; it also appears extensively in vernacular construction, especially in retaining walls erected for agricultural or traffic purposes in rural settings [2]. In many of these cases, either the original assembly was constructed without mortar or the weak bonding materials deteriorated, resulting in structures that function effectively as dry-joint assemblies [3–5].

These dry-joint structures, often recognized for their cultural and historical value, are primarily subjected to their own weight and ground pressure, which means they are generally designed to carry compressive loads. However, due to their quasi-brittle

behavior and lack of tensile strength [6], dry-joint structures, particularly retaining walls, are vulnerable to failure under out-of-plane loads [7]. As a result, there has been a growing research interest in understanding the behavior of dry-joint structures, especially focusing on how they respond to different loading conditions [8–17], and, in particular, the dry-joint response [18–20].

Dry-joint masonry structures pose unique challenges because they rely heavily on the mechanical properties of their individual contact points. Studies have shown that joint failure can greatly impact the non-linear response of these structures, especially in out-of-plane loading scenarios [17,21]. For example, Santa-Cruz et al. [1] used a numerical approach based on a Mohr–Coulomb failure criterion to investigate the effects of joint irregularities, finding that joint stiffness and friction angle directly influence structural stability. Savalle et al. [22], in another numerical study, examined the seismic in-plane behavior of eight dry-joint walls, demonstrating that joint stiffness affects both the ultimate load-bearing capacity and the failure mechanism.

Despite these insights, there remains a lack of experimental data on the stiffness and variability of dry joints. Variability in joint properties complicates predictions and assessments; for example, ref. [20] reported up to 30% variation in stone stiffness, while Vlachakis et al. [18] and Colombo et al. [23] found significant scatter in stiffness measurements across different stones. This variability has profound implications, as it affects the response and stability of structures subjected to seismic or other dynamic forces, which are increasingly relevant in modern contexts where historical preservation and adaptation are essential.

The methodology in this paper seeks to address gaps in the current understanding of dry-joint structures by experimentally investigating the out-of-plane response across different configurations and stone types. Unlike prior studies that primarily focused on single joints or large structures joint analyses, this study examines the global behavior of larger assemblies and the intermediate (3 to 5 blocks) structures and aims to capture any averaging effects across multiple joints. Additionally, the experimental program includes three different stone types with varying morphologies to account for material heterogeneity—a factor often underrepresented in modeling but significant for real-world applications. By loading these assemblies up to collapse on a tilting table, this study provides insights into failure mechanisms that can guide conservation efforts for heritage structures and inform the design of new structures in seismic regions.

This paper is organized as follows: Section 2 describes the materials and experimental setup used to replicate the loading conditions on dry-joint structures, simulating forces such as seismic activity or wind load. Section 3 presents and analyzes the results of the experimental campaign, including failure mechanisms and load–displacement behavior. Finally, this paper concludes with a discussion of the implications of these findings for both historical preservation and contemporary engineering applications, as well as potential directions for future research.

Masonry structures, particularly dry-joint assemblies, are uniquely resilient yet vulnerable. Their resilience lies in the strength of gravity-driven self-weight loads, while their vulnerability stems from the absence of tensile bonding, which limits their performance under dynamic forces. Over the years, dry-joint masonry has been widely recognized for its sustainability, durability, and adaptability, especially in seismically active regions. However, the unpredictable behavior of dry joints under various loading conditions, such as seismic events, poses challenges for both heritage preservation and modern applications. In the absence of bonding materials, dry-joint structures depend heavily on the mechanical properties of stone interfaces, which are influenced by factors like material composition, stone morphology, and the variability of contact surfaces. Consequently, the response of these structures under loads such as lateral forces, ground motion, and wind is far from uniform, making it essential to investigate joint behavior across diverse configurations and conditions.

Previous studies have highlighted the complexities of dry-joint behavior through experimental and numerical approaches, providing insights into factors such as joint stiffness, friction angle, and out-of-plane response. Yet, there remains a substantial gap

in quantifying the real-world variability and heterogeneity of joint properties, which can differ greatly even within a single structure. This study builds upon existing knowledge by adopting a systematic experimental approach that accounts for the natural irregularities in stone morphology and examines the global response of dry-joint structures across different assembly configurations. By utilizing three distinct types of stones and testing assemblies with increasing block numbers, this study seeks to capture the averaging effects of joint variability on structural stability, aiming to offer data-driven insights that can inform both historical conservation and contemporary engineering practices. Ultimately, this study's findings aim to bridge gaps between the theoretical, experimental, and practical understanding of dry-joint masonry, with implications for enhancing the resilience of these structures under dynamic loads.

## 2. Experimental Program

### 2.1. Materials

In this study, three types of stones are analyzed: volcanic stones from the northern part of Garrotxa (Figure 1a), sedimentary stones from Alt Empordà (Figure 1b), and artificial concrete blocks prepared for the tests (Figure 1c). The volcanic stones from the northern part of Catalunya (Garrotxa) are very irregular in terms of morphology with random dimensions. In addition, these stones are significantly porous and belong to the Pyroclastic family of stones. The sedimentary stones are metamorphic rocks, mainly composed of schist and licorella formed out of feldspars decomposition. The stones' shape is relatively squared and plane, although the dimensions are quite irregular. Finally, the concrete blocks (artificial stone) samples are the most regular ones, with standard dimensions of 250 mm × 125 mm × 100 mm. The last dimension (100 mm) corresponds to the height of the masonry courses for the masonry assemblies. The surfaces of these blocks are not completely flat and have some imperfections, which will, according to the literature, play a role in the contacting interfaces and, therefore, in the dry-joint stiffness [18]. Densities read 28 kN/m<sup>3</sup>, 25 kN/m<sup>3</sup>, and 22 kN/m<sup>3</sup> for the volcanic stones, the sedimentary stones, and the concrete parallelepipedal units, respectively.



**Figure 1.** Different stones investigated: (a) volcanic stones from Garrotxa; (b) sedimentary stones from Empordà; and (c) concrete parallelepipedal units.

### 2.2. Test Setup

The experimental campaign uses the principle of the tilting table and its capacity to study the collapse mechanisms of masonry structures [24]. Historically, it has been a tool to understand their behavior and collapse mechanisms [9,12,15,16,25–27]. Despite the simplicity of the test, it estimates the horizontal collapse load multipliers of structures and makes it possible to observe the associated failure mechanisms [23,27–29].

When the table tilts, the self-weight of the structure is gradually converted into an increasing horizontal force, simulating external actions such as seismic activity or wind loads, up to the collapse, for a given angle, denoted as  $\alpha$ , at which structural equilibrium is no longer maintained. The load multiplier in structural mechanics is a scalar factor that indicates the proportional increase in load, with respect to the self-weight, required to cause failure. It is a fundamental parameter of limit analysis (LA) theorems [30–33]. For tilting tests, the load multiplier  $\lambda$  is simply determined by calculating the ratio of the horizontal

collapse load  $H$  to the vertical load (self-weight)  $W$ , which gives  $\lambda = H/W$  or, alternatively,  $\lambda = \tan \alpha$ .

Actual structures (mainly retaining walls) in the Garrotxa zone need to sustain seismic activity due to volcanos and loads due to the infill, while structures in Alt Empordà are subjected to strong wind actions and loads due to the infill, as well. These loading scenarios consist of horizontal forces that can be recreated through a tilting table setup in order to reproduce the local failure mechanisms. In addition to the evaluation of the collapse angle, the tilting table setup also allows for obtaining the coefficient of friction ( $\mu$ ) of the material interfaces. Yet, the interface is characterized by the unique presence of self-weight loads, as the type of contact between these irregular stones does not allow the use of a more complex test setup to determine the coefficient of friction ( $\mu$ ).

The tilting table used in this work consists of a wooden platform supported by a steel frame (Figure 2). The wooden platform has a mechanism to fix the bottom of the structures and constrain their horizontal displacement. The steel frame is then hooked to a steel wire that is raised through a motor controlled by a dedicated program to ensure a repeatable procedure with a tilting speed of  $0.5^\circ/\text{s}$ . An inclinometer is installed into the tilting table to obtain the collapse angle, and a camera records the experiment to read the perfect collapse angle from the slow-motion videos.

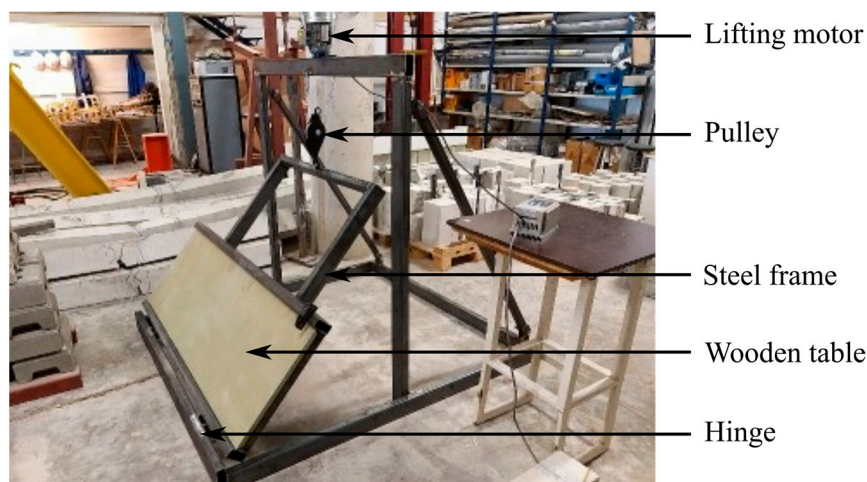


















**Figure 2.** Tilting table setup developed at University of Girona.

### 2.3. Tests Configuration

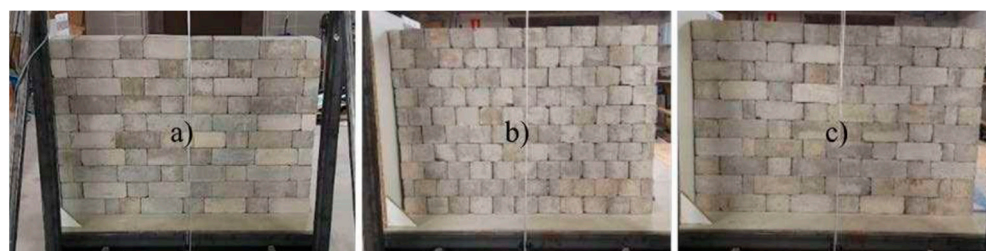
The experimental campaign is composed of two sets of tests: (i) dry-joint structures and ii) dry-joint full walls. The first one consists of an assembly of 2, 3, 4, or 5 stacked blocks (Table 1). For the concrete blocks, the erected columns are positioned either perpendicularly or parallelly (see concrete parallel and perpendicular in Table 1) to the tilting axis. In the case of volcanic (Garrotxa) and sedimentary (Alt Empordà) stones, due to their irregular shape, it is not possible to discriminate between perpendicular or parallel orientation. Hence, only one configuration is tested, where larger (stones with larger contact area) stones are placed at the bottom, and the smaller ones are placed at the top. The structures are then tilted up to their collapse, either by sliding or overturning mode. For each type of stone and for each structure type (2, 3, 4, and 5 blocks), three sets of stones are chosen and tested 10 times each, resulting in 30 tests for each assembly.



**Table 1.** Representative collapse modes for tests with 2, 3, 4, and 5 courses of each type of stone.

Stone type	2 courses	3 courses	4 courses	5 courses
Concrete (parallel)				
Concrete (perpendicular)				
Garrotxa				
Alt Empordà				

The second set of tests (dry-joint full walls) consists of an assembly of 140 units of concrete blocks, resulting in a 1 m high, 1.46 m long, and 0.25 m thick wall. Three different configurations with different ratios of headers and stretchers [27–29] are tested three times each for repeatability purposes (Figure 3). Configuration A (Figure 3a) consists of 10 courses of 11 entire stones (250 mm × 125 mm × 100 mm) and two stones cut in thirds (83 mm × 125 mm × 100 mm). All the pieces are placed cutting the joints. Configuration B (Figure 3b) consists of 10 courses of 11 entire blocks for the odd courses and 10 entire blocks plus two half blocks (dimensions: 250 mm × 62 mm × 100 mm) at the extremes for the even courses. All the stones are placed as headers. Finally, configuration C (Figure 3c) is similar to configuration A but has the headers placed at different locations.

**Figure 3.** Second set of tests (dry-joint full walls) with assembly of concrete units to build a whole wall: (a) configuration A; (b) configuration B; (c) and configuration C.

### 3. Results and Discussions

#### 3.1. Small Tests (Dry-Joint Structures)

In this section, the experimental results of the first set of tests (dry-joint structures) are presented and analyzed. Results corresponding to tests on two, three, four, and five courses, volcanic (Garrotxa), sedimentary (Empordà) stones, and artificial concrete blocks, are presented in Table 2. For every assembling configuration of two to five courses, a total of 30 tests for concrete blocks and 39 for Garrotxa and Alt Empordà stones are performed, which are grouped in Table 2 according to their collapse mode (i.e., sliding or toppling) so that variable  $n$  refers to the number of occurrences of each failure mode. Here,  $\bar{\alpha}$  refers to the mean value of the angle of collapse (in degrees),  $\sigma_{\alpha}$  refers to the standard deviation (in degrees), and finally, CoV refers to the coefficient of variation. Variable  $n$  refers to the number of occurrences of each failure mode.

**Table 2.** Experimental results of the first series of dry-joint structures. *Following the same order of Table 1: Concrete Blocks in parallel disposition, concrete blocks in perpendicular disposition, Garrotxa stones and Alt Empordà stones.*

Stacked Pieces	Collapse Mode	Concrete Blocks in parallel disposition				Concrete blocks in perpendicular disposition				Garrotxa stones				Alt Empordà stones			
		n	$\bar{\alpha}$	$\sigma_{\alpha}$	CoV (%)	n	$\bar{\alpha}$	$\sigma_{\alpha}$	CoV (%)	n	$\bar{\alpha}$	$\sigma_{\alpha}$	CoV (%)	n	$\bar{\alpha}$	$\sigma_{\alpha}$	CoV (%)
2	Sliding	22	30.8	1.8	6	28	33.3	2.8	8	29	23.1	4.9	21	39	40	2.8	7
	Toppling	8	31.3	1.9	6	2	33.3	1.3	4	10	37.7	7.6	20	0	-	-	-
3	Sliding	0	-	-	-	30	32.6	1.3	4	4	26.6	6.5	24	39	34.2	2.9	8
	Toppling	30	23.1	0.6	2	0	-	-	-	35	30	4.1	14	0	-	-	-
4	Sliding	0	-	-	-	10	31.8	0.8	3	13	21.1	4.5	21	31	33.9	2.7	8
	Toppling	30	16.7	1.4	8	20	31.1	1.1	4	19	22.6	4.9	22	8	30.7	2.9	9
5	Sliding	0	-	-	-	0	-	-	-	6	17.1	7.1	41	28	27.8	4.1	15
	Toppling	30	13.1	0.9	7	30	26.6	0.4	2	33	17.7	5.6	31	11	27.3	4.5	17

For the concrete blocks in the parallel configuration, sliding failure mode takes place only in the case of two-stacked pieces. For a larger number of stacked pieces, toppling is the prevalent failure mode, and it happens at a reduced inclination angle. The same occurs with the perpendicular configurations but at a higher angle. Independently of the configuration (parallel or perpendicular), the sliding failure always occurs at the same angle. Secondly, in both cases of concrete blocks (parallel and perpendicular), repeatability is always characterized by a coefficient of variation lower than 10%. However, it is worth noting that, for given assemblies, noticeable differences (sliding and overturning failures) are obtained between the different contacts. Toppling failure is more likely in the parallel configuration due to the smaller width, which causes the resultant force at the center of gravity to reach a point outside the base more quickly.

For the Garrotxa and the Alt Empordà stones, similar conclusions can be drawn, yet with an expected greater difference between the different natural interfaces. Overall, one can notice a significant difference between the Garrotxa and Alt Empordà stones. Both types of stones display a decreasing trend in terms of angle of collapse, which is greater on Alt Empordà stones due to their surface morphology. The results of the Alt Empordà stones are comparable to the concrete blocks with perpendicular configuration, with a slightly higher coefficient of variation (~8% compared with ~5%), but above all, consistent mechanisms with mostly sliding for two- and three-block assemblies and toppling that appear afterward; the discrepancies are due to the difference in aspect ratios between the units. On the contrary, the behavior of the Garrotxa stones, given their particular and heterogeneous shapes, displays much more variability and shows significantly more toppling failure for three-stone than for four-stone assemblies, which

would not be expected. The behavior of such assemblies is therefore very dependent on the selected blocks and positions.

It is worth noting that concrete blocks, which have a much flatter surface shape, have a lower friction coefficient than the natural Alt Empordà stones. This can be attributed to the imperfections of the surface.

As a general observation in tests that failed by sliding, the collapse angle decreases as the number of stacked blocks increases, especially for natural stones (Table 2). This trend can be explained by the progressive inclination of each stone layer, which alters the decomposition of gravitational forces, generating both perpendicular and parallel components at each joint. According to the limit state theory in masonry structures [31], this decomposition increases the cumulative sliding forces across successive joints, ultimately reducing the sliding capacity of the entire assembly. As a result, the structure reaches collapse at lower angles of inclination due to the greater cumulative sliding forces and the lack of bonding between units, leading to structural instability.

### 3.2. Large Tests (Dry-Joint Full Walls)

Table 3 shows the results of the second series of tests (dry-joint full walls) for the three tested configurations. Following the strategy in Table 2, variable  $n$  refers to the number of occurrences of each failure mode,  $\bar{\alpha}$  refers to the mean value of the angle of collapse,  $\sigma_{\alpha}$  refers to the standard deviation, and finally, CoV refers to the coefficient of variation. First, given the slenderness of the structure, only toppling failure is experimentally observed. The same phenomena as on the small tests are observed: the slenderness helps the resultant force reach an out-of-base projected point sooner. As expected, configurations A and C have the same collapse angle. In addition, they display similar collapse mechanisms with an “inclined” failure line [27] (Figure 4). Configuration B, on the contrary, has a slightly higher collapse angle and a horizontal failure line constrained by the headers in the whole wall (Figure 4). Therefore, as noted by other authors [10,28,29,31], the more headers, the bigger the angle of collapse the structure will reach. In this sense, and according to experimental results presented, the change from configuration A/C to configuration B corresponds to a difference in collapse angle of  $0.8^{\circ}$  ( $<10\%$ ), which makes it very difficult for the authors to reach a conclusion with a significant difference. More interestingly, the variability of the global response seems smaller than for the small assemblies of the first set of tests (standard deviation of  $0.3^{\circ}$  (2.5%) on average for the full structure compared with  $1.2^{\circ}$  (4.75%) on average for the small-scale tests. This is a sign that multiple interfaces (in the length of the wall) average their global behavior, leading to a more repeatable (and therefore robust) wall.

**Table 3.** Experimental results of the second series of dry-joint full walls.

Configuration			Dry-Stone Full Wall		
Configuration	Collapse Mode	n	$\bar{\alpha}$	$\sigma_{\alpha}$	CoV (%)
A	Sliding	0	-	-	-
A	Toppling	3	10.8	0.2	2
B	Sliding	0	-	-	-
B	Toppling	3	11.6	0.3	2
C	Sliding	0	-	-	-
C	Toppling	2	10.9	0.4	3

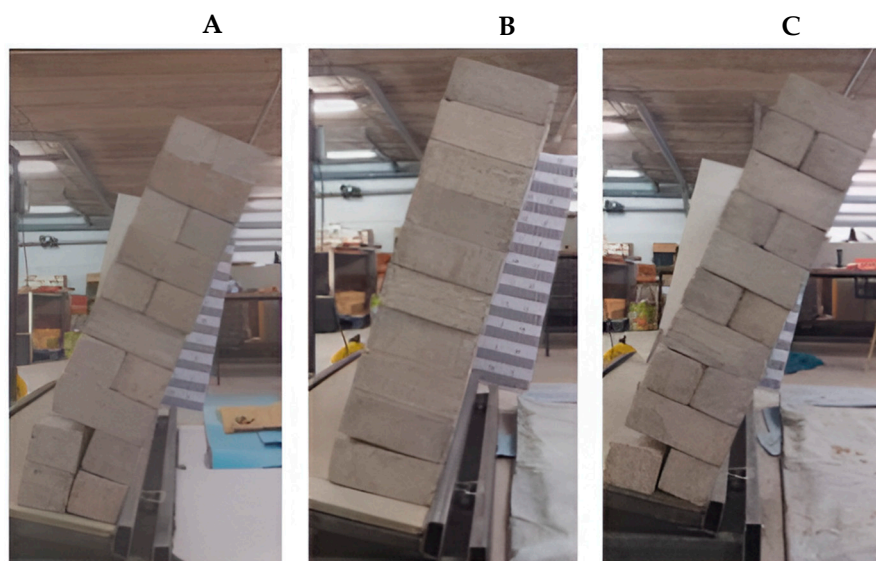


**Figure 4.** Representative collapse modes for dry-joint full wall tests with (A) configuration A, (B) configuration B, and (C) Configuration C.

#### 4. Conclusions

This study presents a comprehensive analysis of the mechanical behavior of dry-stone masonry structures, particularly focusing on the out-of-plane collapse mechanisms under pseudo-static loading conditions. Through experimental analyses on both small assemblies and full-wall dry-stone structures, several key insights and outcomes were identified.

1. **Influence of Stone Geometry and Morphology:** The experiments confirm that collapse behavior in dry-stone structures is highly dependent on stone morphology, arrangement, and number of layers. Stones from different regions, specifically volcanic stones from Garrotxa and sedimentary stones from Alt Empordà, exhibit distinct failure patterns. Variability in natural stone shape and surface irregularities causes differences in collapse angles, with smoother surfaces (as seen in concrete blocks) leading to a lower coefficient of friction and altered failure patterns.
2. **Failure Mechanisms in Small Assemblies:** For assemblies with fewer blocks, sliding failure was observed predominantly, especially when frictional resistance at the joints was insufficient. As the number of layers increased, toppling failure became more common due to the gravitational center shifting outside the base area. This outcome aligns with theoretical expectations, reinforcing the role of joint morphology in out-of-plane stability. Interestingly, the angle of collapse for sliding failures decreased with an increase in block layers, attributed to the cumulative sliding forces distributed across joints in successive layers.
3. **Large Assemblies and Wall Structures:** In larger assemblies, such as the full-wall configurations, only toppling failures were observed, underscoring that slender wall structures are more susceptible to overturning than sliding. Configurations with more headers (horizontal blocks) demonstrated slightly higher angles of collapse, indicating a stabilizing effect due to better horizontal resistance. This finding aligns with other studies that also suggest that walls with consistent headers and stretchers provide improved stability under lateral forces.
4. **Material Heterogeneity:** This study highlights the significant impact of material heterogeneity on structural performance. Variability in joint friction and surface morphology introduces considerable dispersion in failure angles, especially in natural stones. This variability supports the use of friction-based failure models in future simulations, as traditional models might not fully capture the nuances of these heterogeneities. Understanding these dynamics is essential for accurately predicting and designing the behavior of dry-stone structures.



5. Implications for Heritage and Seismic Regions: Given the findings, this study has valuable implications for both historical preservation and the design of new structures in seismic areas. Understanding the variability and mechanical interaction between stone units can inform strategies to improve the stability of heritage structures. It also highlights the importance of joint contact mechanics and material variability, which are crucial for enhancing the resilience of dry-stone constructions against dynamic forces such as seismic loads.

**Future Directions:** Future research should focus on refining numerical models that account for irregular stone morphology and joint behavior to better simulate real-world conditions. Expanding the range of stone types and configurations tested could further validate and enrich the observed trends. Additionally, exploring the influence of dynamic loading conditions, such as varying seismic forces, on dry-stone assemblies will provide deeper insights into their stability and inform preservation efforts for historic masonry structures.

**Supplementary Materials:** The following supporting information can be downloaded at: <https://www.mdpi.com/article/10.3390/buildings14123744/s1>, Assaigs  $\mu$  i Llicament\_Bolc (ENG:  $\mu$  test for sliding and toppling).

**Author Contributions:** Conceptualization, I.C. and J.L.; methodology, I.C. and N.S.; validation, N.S., J.L., J.S., E.G., J.F. and M.À.C.; formal analysis, I.C. and N.S.; investigation, I.C., J.L. and M.À.C.; resources, J.L. and N.S.; data curation, I.C. and N.S.; writing—original draft preparation, I.C.; writing—review and editing, J.L. and N.S.; visualization, I.C.; supervision, J.L.; project administration, J.L., J.S. and M.À.C.; funding acquisition, J.L., M.À.C., J.S., J.F. and E.G. All authors have read and agreed to the published version of the manuscript.

**Funding:** This research was funded by the *PECT Girona Patrimoni Actiu* program [grant number 001-P-000916], and the APC was funded by the University of Girona (UdG).

**Data Availability Statement:** Data fully available within the article or its supplementary material.

**Conflicts of Interest:** The authors declare no conflict of interest.

## References

1. Bui, T.T.; Limam, A.; Sarhosis, V.; Hjiat, M. Discrete element modelling of the in-plane and out-of-plane behaviour of dry-joint masonry wall constructions. *Eng. Struct.* **2017**, *136*, 277–294. [[CrossRef](#)]
2. Savalle, N.; Monchal, C.; Vincens, E.; Forcioli, S.; Lourenço, P.B. Static and seismic design of Dry-Stone Retaining Walls (DSRWs) following Eurocode standards. *Eng. Struct.* **2023**, *274*, 114847. [[CrossRef](#)]
3. Smoljanović, H.; Živaljić, N.; Nikolić, Ž. A combined finite-discrete element analysis of dry-stone masonry structures. *Eng. Struct.* **2013**, *52*, 89–100. [[CrossRef](#)]
4. Roca, P.; Cervera, M.; Gariup, G. Structural analysis of masonry historical constructions. Classical and advanced approaches. *Arch. Comput. Methods Eng.* **2010**, *17*, 299–325. [[CrossRef](#)]
5. Paulo, P.R.G.; Lourenço, B. *Angelo, Historic Construction and Conservation: Materials, Systems and Damage*; Routledge: New York, NY, USA, 2019. [[CrossRef](#)]
6. Vasconcelos, G.; Lourenço, P.B. In-plane experimental behavior of stone masonry walls under cyclic loading. *J. Struct. Eng.* **2009**, *135*, 1269–1277. [[CrossRef](#)]
7. Bruneau, M. Seismic evaluation of unreinforced masonry buildings—A state-of-the-art report. *Can. J. Civ. Eng.* **1994**, *21*, 512–539. [[CrossRef](#)]
8. de Buhan, P.; de Felice, G. A homogenization approach to the ultimate strength of brick masonry. *J. Mech. Phys. Solids* **1997**, *45*, 1085–1104. [[CrossRef](#)]
9. Alejano, L.R.; Veiga, M.; Gómez-Márquez, I.; Taboada, J. Stability of granite drystone masonry retaining walls: II. Relevant parameters and analytical and numerical studies of real walls. *Géotechnique* **2012**, *62*, 1027–1040. [[CrossRef](#)]
10. Casapulla, C.; Maione, A. Experimental and analytical investigation on the corner failure in masonry buildings: Interaction between rocking-sliding and horizontal flexure. *Int. J. Archit. Herit.* **2018**, *14*, 208–220. [[CrossRef](#)]
11. Colas, A.-S.; Morel, J.-C.; Garnier, D. Assessing the two-dimensional behaviour of drystone retaining walls by full-scale experiments and yield design simulation. *Géotechnique* **2013**, *63*, 107–117. [[CrossRef](#)]
12. Colas, A.-S.; Morel, J.-C.; Garnier, D. Full-scale field trials to assess dry-stone retaining wall stability. *Eng. Struct.* **2010**, *32*, 1215–1222. [[CrossRef](#)]

13. Ita, P.; Santa-Cruz, S.; Daudon, D.; Tarque, N.; Párraga, A.; Ramos, V. Out-of-plane analysis of dry-stone walls using a pseudo-static experimental and numerical approach in natural-scale specimens. *Eng. Struct.* **2023**, *288*, 116153. [[CrossRef](#)]
14. Mundell, C.; McCombie, P.; Heath, A.; Harkness, J. Behaviour of drystone retaining structures. *Proc. Inst. Civ. Eng. (Struct. Build.)* **2010**, *163*, 3–12. [[CrossRef](#)]
15. Portioli, F.; Cascini, L. Assessment of masonry structures subjected to foundation settlements using rigid block limit analysis. *Eng. Struct.* **2016**, *113*, 347–361. [[CrossRef](#)]
16. Vélez, L.F.R.; Magenes, G.; Griffith, M.C. Dry stone masonry walls in bending—Part I: Static tests. *Int. J. Archit. Herit.* **2014**, *8*, 1–28. [[CrossRef](#)]
17. Santa-Cruz, S.; Daudon, D.; Tarque, N.; Zanelli, C.; Alcántara, J. Out-of-plane analysis of dry-stone walls using a pseudo-static experimental and numerical approach in scaled-down specimens. *Eng. Struct.* **2021**, *245*, 112875. [[CrossRef](#)]
18. Villemus, B.; Morel, J.-C.; Boutin, C. Experimental assessment of dry stone retaining wall stability on a rigid foundation. *Eng. Struct.* **2006**, *29*, 2124–2132. [[CrossRef](#)]
19. Vlachakis, G.; Colombo, C.; Giouvanidis, A.I.; Savalle, N.; Lourenço, P.B. Experimental characterisation of dry-joint masonry structures: Interface stiffness and interface damping. *Constr. Build. Mater.* **2023**, *392*, 130880. [[CrossRef](#)]
20. Kulatilake, P.; Shreedharan, S.; Sherizadeh, T.; Shu, B.; Xing, Y.; He, P. Laboratory estimation of rock joint stiffness and frictional parameters. *Geotech. Geol. Eng.* **2016**, *34*, 1723–1735. [[CrossRef](#)]
21. Oliveira, R.L.; Rodrigues, J.P.C.; Pereira, J.M.; Lourenço, P.B.; Marschall, H.U. Normal and tangential behaviour of dry joints in refractory masonry. *Eng. Struct.* **2021**, *243*, 112600. [[CrossRef](#)]
22. Savalle, N.; Lourenço, P.B.; Milani, G. Joint Stiffness Influence on the First-Order Seismic Capacity of Dry-Joint Masonry Structures: Numerical DEM Investigations. *Appl. Sci.* **2022**, *12*, 2108. [[CrossRef](#)]
23. Colombo, C.; Savalle, N.; Mehrotra, A.; Funari, M.F.; Lourenço, P.B. Experimental, numerical and analytical investigations of masonry corners: Influence of the horizontal pseudo-static load orientation. *Constr. Build. Mater.* **2022**, *344*, 127969. [[CrossRef](#)]
24. Colombo, C.; Savalle, N.; Funari, M.F.; Vlachakis, G.; Giouvanidis, A.I.; Karimzadeh, S.; Lourenço, P.B. Experimental investigation of the horizontal load orientation on masonry corner failure. *Int. J. Mason. Res. Innov.* **2024**, *9*, 313–330. [[CrossRef](#)]
25. Colombo, C.; Fernandes, L.; Savalle, N.; Lourenço, P.B. Tilting tests for masonry structures: Design and preliminary numerical modeling. In Proceedings of the 14th Canadian Masonry Symposium, Montreal, QC, Canada, 17–20 May 2021; pp. 1–11.
26. Shi, Y.; D’Ayala, D.; Prateek, J. Analysis of out-of-plane damage behaviour of unreinforced masonry walls. In Proceedings of the 14th International Brick and Block Masonry Conference, Sydney, Australia, 13–20 February 2008; pp. 2–17.
27. Savalle, N.; Vincens, E.; Hans, S. Pseudo-static scaled-down experiments on dry stone retaining walls: Preliminary implications for the seismic design. *Eng. Struct.* **2018**, *171*, 336–347. [[CrossRef](#)]
28. de Felice, G. Out-of-plane seismic capacity of masonry depending on wall section morphology. *Int. J. Archit. Herit.* **2011**, *5*, 466–482. [[CrossRef](#)]
29. Felice, G.D.; Giannini, R. Out-of-plane seismic resistance of masonry walls. *J. Earthq. Eng.* **2001**, *5*, 253–271. [[CrossRef](#)]
30. Alejano, L.R.; Muralha, J.; Ulusay, R.; Li, C.C.; Pérez-Rey, I.; Karakul, H.; Chryssanthakis, P.; Aydan, Ö. ISRM Suggested Method for Determining the Basic Friction Angle of Planar Rock Surfaces by Means of Tilt Tests. *Rock Mech. Rock Eng.* **2018**, *51*, 3853–3859. [[CrossRef](#)]
31. Lourenço, P.B.; Roca, P. Limit Analysis of Masonry Structures with Unreinforced and Confined Walls. *J. Struct. Eng.* **1997**, *123*, 1030–1039.
32. Heyman, J. *The Stone Skeleton: Structural Engineering of Masonry Architecture*; Cambridge University Press: Cambridge, UK, 1996.
33. Savalle, N.; Vincens, É.; Hans, S. Experimental and numerical studies on scaled-down dry-joint retaining walls: Pseudo-static approach to quantify the resistance of a dry-joint brick retaining wall. *Bull. Earthq. Eng.* **2020**, *18*, 581–606. [[CrossRef](#)]

**Disclaimer/Publisher’s Note:** The statements, opinions and data contained in all publications are solely those of the individual author(s) and contributor(s) and not of MDPI and/or the editor(s). MDPI and/or the editor(s) disclaim responsibility for any injury to people or property resulting from any ideas, methods, instructions or products referred to in the content.